

flexibility arises by virtue of the arbitrariness of the operators H^0 , \mathcal{L}^0 which are to be chosen in each instance so that the significant parts of the mathematical spectrum of H^0 , \mathcal{L}^0 are most simply associated with their physical counterparts. In some instances this "mapping" procedure becomes a matter of personal taste. The choice which is obviously "most physical" to one person is not always so evident to someone else.

In the applications given here we have usually employed R -matrix-type boundary conditions for the operator \mathcal{L}^0 , the reasons for this choice being discussed already in I. Nevertheless, the formalism allows for multiple choices of the basic operators and only after a careful evaluation of each choice will it be possible to decide which choice is most appropriate for the particular problem being investigated. General criteria for

choosing a set of operators are not obvious due to the necessity of compromising between mathematical convenience and "physical" significance. Fortunately, many of the interesting results may be obtained without specifying H^0 and \mathcal{L}^0 too precisely so that the basic formalism is reasonably universal in its applicability to nuclear reactions. Applications of the formalism to direct reactions and nuclear-model calculations will be reported at a later time.

ACKNOWLEDGMENT

One of us (D. R.) would like to acknowledge the hospitality of the United Kingdom Atomic Energy Research Establishments, which provided financial support and facilities necessary for part of this work.

$^{14}\text{N}(^{14}\text{N},^{13}\text{N})^{15}\text{N}$ Reaction at Low Energies and the Elastic Scattering of ^{14}N by $^{14}\text{N}^\dagger$

G. BREIT, J. A. POLAK, AND D. A. TORCHIA

Yale University, New Haven, Connecticut

(Received 24 April 1967)

The molecular-viewpoint form of nucleon tunneling theory is used in the two-level approximation and with neglect of the dynamic reaction terms for a partial-wave analysis allowing the inclusion of the effects of wave function absorption through the use of an imaginary part of the potential. The equations are used in an analysis of improved measurements of the differential and total cross sections of the reaction $^{14}\text{N}(^{14}\text{N},^{13}\text{N})^{15}\text{N}$, with special attention to laboratory energies $E_{\text{lab}} \leq 16$ MeV which are below the Coulomb barrier. At the lowest energies, the analysis involves only the Coulomb interaction between the heavy particles. Fits to data are improved at the higher energies through the introduction of optical potentials. The principal function of these in the present work is to modify the wave function at distances larger than those corresponding to definite contact between ^{14}N and ^{14}N . The transfer function $\beta(R)$ is cut off at small values of the internuclear distance R to avoid the inclusion of unrealistic contributions to neutron transfer when the two nuclei are no longer distinct. The potential has been adjusted for best fits to neutron-transfer data. The long distance tail of the potentials tried was made to agree, regarding relative values at different distances, with that calculated by McIntosh, Rawitscher, and Park in their work on the elastic scattering of ^{14}N by ^{14}N , and depends therefore on nucleon-nucleus scattering information. The potentials were adjusted to represent the elastic-scattering $^{14}\text{N}+^{14}\text{N}$ data simultaneously with neutron-transfer data. These combined requirements are met best by potentials referred to as 2 and 3 in the text. The reduced width of the transferred neutron obtained from transfer data depends on the potential only weakly. The same reduced width from elastic-scattering information is sensitive to the choice of potential. The best agreement of the elastic-scattering and neutron-transfer reduced widths is obtained for potential 3, the disagreement being less than by a factor 2. The combined uncertainty of the two ways of arriving at the reduced width is believed to be large and to make the discrepancy insignificant. The combined treatment of neutron transfer and of elastic scattering is self-consistent in the sense described. The neutron transfer reduced width is slightly smaller than the single-particle reduced width calculated with the nucleon-nucleus potential employed in obtaining the proportionality constant of the long-distance nucleus-nucleus potential tail.

I. INTRODUCTION

THE treatment of nucleon tunneling proposed by one of the writers¹⁻³ is applied to the analysis of the $^{14}\text{N}(^{14}\text{N},^{13}\text{N})^{15}\text{N}$ reaction data of Becker and

McIntyre,⁴ of Hiebert, McIntyre, and Couch⁵ as well as Gaedke, Toth, and Williams.⁵ The treatment, in its main part, avoids schematic and questionable replacements of many particle systems by single particles or

[†] This research was supported by the U. S. Atomic Energy Commission under Contract No. AT(30-1)-1807 (Report No. Yale-1807-44), by the U. S. Army Research Office-Durham, and by the U. S. Air Force of Scientific Research, Office of Aerospace Research, under AFOSR Grant No. AF 394-66.

¹ G. Breit, in *Proceedings of the Conference on Direct Interactions and Nuclear Reaction Mechanisms, Padua, 1962*, edited by E. Clementel and C. Villi (Gordon and Breach Science Publishers, Inc., New York, 1963), p. 1.

² G. Breit, in *Proceedings of the Third Conference on Reactions Between Complex Nuclei*, edited by A. Ghiorso, R. M. Diamond, and H. E. Conzett (University of California Press, Berkeley, California, 1963), p. 97.

³ G. Breit, *Phys. Rev.* **135**, B1323 (1964).

⁴ L. C. Becker and J. A. McIntyre, *Phys. Rev.* **138**, B339 (1965).

⁵ J. C. Hiebert, J. A. McIntyre, and J. G. Couch, *Phys. Rev.* **138**, B346 (1965), referred to as HMC; R. M. Gaedke, K. S. Toth, and I. R. Williams, *ibid.* **141**, 996 (1966), referred to as GTW.

cores. The neutron-emitting and neutron-receiving nuclei are each considered^{1-3,6} somewhat along the lines of an electrical engineer's "black box" characterized by its response to external stimuli by means of quantities related to, though not identical with, the reduced widths of Wigner's \mathcal{R} -matrix theory. The limitations of the general theory have been discussed in Ref. 3.

The extension of the data to lower energies in Refs. 4 and 5 has proved especially valuable in providing a possibility of a quantitative test of the theory because the energies are definitely below the nominal Coulomb barrier, so that the participation of collisions involving direct contact of nuclear surfaces and therefore of processes of the compound nucleus type is subordinated. Virtual processes^{3,6} may result in moderate enlargements of the effective values of nuclear radii that enter the formula for the cross section of the single neutron-transfer reaction. With the new data^{4,5} there is a considerable margin of safety in this respect, the classical distance of closest approach for motion in a Coulomb field being 8.8 F at an incident energy of 16 MeV as compared with a separation required for contact of 7.2 F, the latter corresponding to a nuclear radius $b=r_0A^{1/3}$ with the rather large value $r_0=1.5$ F, and the data extending to incident energies as low as 11 MeV.

It has been thought probable⁷⁻⁹ that virtual Coulomb excitation (VCE) complicates the neutron-transfer process even apart from affecting the effective value of the nuclear radius, some early estimates having indicated that it might cause an appreciable enhancement of the transfer probability for distant collisions. The particular effect which appeared most likely to cause the complication has been shown however to be very small¹⁰ and there appears to be no reason for expecting a large direct effect of VCE on the transfer probability in the case of distant collisions. The theory of the tunneling process for the reaction under consideration has some omissions, however, such as an incomplete consideration of the nucleon configurations of the participation of a larger number of states and the neglect of the dynamic reaction terms.^{1,3} The VCE process may be affecting other reactions¹¹ and through them the force between the colliding nuclei. The neutron- and proton-transfer reactions themselves also have an effect on this force. The complexity of these effects makes the data analysis at the higher energies necessarily somewhat phenomenological. At the lowest available energies the smallness of the reaction yield decreases the experi-

mental accuracy. Nevertheless, a comparison of the observed angular distributions with calculations making use of the imperfect theory of pure tunneling appears useful since it gives an idea of the magnitude of the effects to be accounted for in improved versions of the theory. The comparison is carried out in more detail in the present paper than in Ref. 8 and Ref. 12. Inasmuch as the forces between the heavy nuclei are allowed to be not purely Coulomb, the possibility of reactions other than the single neutron transfer is partly allowed for, and later more complete experimental data are used.

The inclusion of other than purely Coulomb forces is described in Sec. II, which contains also a discussion of the way in which the present treatment is combined with the "molecular" viewpoint¹⁻³ of the tunneling process. In order to include incident laboratory energies as high as 16 and 18 MeV, the motion of the nuclei is described by means of a complex potential somewhat as in the optical-model discussions of nuclear reactions. The main difference from the latter is that the calculation of the reaction probability takes place by means of the equations derived from the molecular, "two black boxes," viewpoint. These two ingredients would be irreconcilable if the potential used were to produce an appreciable interpenetration of the two nuclei. It was found possible, however, to obtain satisfactory fits to experiment by means of potentials which are only slightly attractive but, on account of the centrifugal barrier, are effectively repulsive in those states of relatively high L that are responsible for the main contributions to the reaction cross section. The main rôle of the imaginary part of the potential in the calculations presented below is to take into account the attenuation of the incident wave for internuclear distances corresponding to little overlap of nuclear matter. Since for such positions a description of the incident state in terms of space attenuated waves has a clear meaning, the employment of the imaginary part of the nucleus-nucleus potential to be described below does not interfere in a major way with the consistency of the application of the "two black boxes" viewpoint.

It has been found possible to adjust the potential so as to give also a satisfactory account of elastic-scattering data in the $^{14}\text{N}+^{14}\text{N}$ collision along the general lines of previous analyses of scattering data by the Yale group,¹³ but with a modification of the short-range part of the interaction. The optical potentials representing the $^{14}\text{N}+^{14}\text{N}$ elastic-scattering data used here as well as in the work just quoted are not purely phenomenological fits to experimental data but make partial use of the

⁶ G. Briet, *Phys. Rev.* **102**, 549 (1956).

⁷ G. Breit and M. E. Ebel, *Phys. Rev.* **103**, 679 (1956). This paper is referred to as BE-I in the text.

⁸ G. Breit, K. W. Chun, and H. G. Wahsweiler, *Phys. Rev.* **133**, B403 (1964). This paper is often referred to as BCW in the text.

⁹ G. Breit and M. E. Ebel, *Phys. Rev.* **104**, 1030 (1956). This paper is referred to as Be-II in the text.

¹⁰ G. Breit, *Proc. Natl. Acad. Sci. U. S.* **57**, 849 (1967).

¹¹ G. Breit, in *Proceedings of the Congrès International de Physique Nucléaire, Paris, 1964* (Editions du Centre National de la Recherche Scientifique, Paris, 1965).

¹² F. C. Jobs and J. A. McIntyre, *Phys. Rev.* **133**, B893 (1964).

¹³ J. S. McIntosh, S. C. Park, and G. Rawitscher, in *Proceedings of the Second Conference on Reactions Between Complex Nuclei*, edited by A. Zucker, F. T. Howard, and E. C. Halbert (John Wiley & Sons, New York, 1960); G. H. Rawitscher, J. S. McIntosh, and J. A. Polak, in *Proceedings of the Third Conference on Reactions Between Complex Nuclei* (University of California Press, Berkeley, 1963), p. 3; J. S. McIntosh, S. C. Park, and G. H. Rawitscher, *Phys. Rev.* **134**, B1010 (1964).

nucleon-nucleus scattering information employing a general connection between phase shift and energy.¹⁴ This connection makes it possible to employ the nucleon-nucleus potential for the computation of the real part of the nucleus-nucleus potential at large inter-nuclear distances. On account of the absence of data on the elastic scattering of ^{13}N by ^{15}N the same potential is used for the initial and final stages of the process. The reduced width derived from neutron transfer and that obtained by fitting the long-distance tail of the elastic-scattering potential are in rough agreement with each other.

Section III describes the procedures used in making fits to data and some of the results. Section IV is concerned with a discussion of the findings, particularly in connection with the limitations of the data analysis.

II. PARTIAL-WAVE ANALYSIS

The partial-wave treatment employed below makes use of Eq. (2.20) of the set of two coupled equations, Ref. 3, which are essentially the same as those presented at the Padua Conference¹ on a previous occasion. The coupled equations are

$$\begin{cases} \left[-\frac{\hbar^2}{2\mu}\Delta_r + \bar{E}^a - E + V_{ab} \right] \bar{\psi}_u - \frac{\hbar^2}{2M}\beta\bar{\psi}_v = 0, \\ \left[-\frac{\hbar^2}{2\mu}\Delta_r + \bar{E}^b - E + V_{ab} \right] \bar{\psi}_v - \frac{\hbar^2}{2M}\beta\bar{\psi}_u = 0. \end{cases} \quad (2.1)$$

The notation is the same as in Ref. 3. The total energy is E ; \mathbf{r} is the vector displacement from the center of mass of nucleus a to that of nucleus b and $r = |\mathbf{r}|$; \bar{E}^a is the energy of the nucleon to be transferred from nucleus a to nucleus b when it is in a ; similarly \bar{E}^b is the energy of the nucleon after it has been transferred to nucleus b ; both of these energies are defined for $r = \infty$ and in each case the arbitrary additive constant in the definition of the energies \bar{E} is adjusted so that $\bar{E} = 0$ for dissociation of a nucleus to a state of rest of the two fragments at an infinite distance between them; V_{ab} is the potential energy describing the relative motion of a and b ; the functions $\bar{\psi}_u$, $\bar{\psi}_v$ are connected with the adiabatic analysis functions ψ^a , ψ^b by the transformations of Eqs. (2.10), (2.11), and (2.13) of Ref. 3; the quantity β contains tunneling penetration factors, is defined in Ref. 7 and is used in the same sense as in Refs. 1, 2, 3, and 8; the reduced mass of the collision process of a and b is denoted by μ , and that of the nucleon by M .

A number of approximations and assumptions are involved in the derivation of (2.1). The equations are supposed to hold if the projectile and target do not come into bodily contact with an appreciable probability. Such is the case at bombarding energies definitely

below the Coulomb barrier. The motion of the nucleon is supposed to be well-enough describable by linear combinations of adiabatic wave functions belonging to two space degenerate states corresponding to the capture of the transferred particle c by a or by b ; certain "dynamic reaction" terms containing the mass ratio M/μ , with M standing for the nucleon mass, were neglected in Eq. (2.17) of Ref. 3 in arriving at Eq. (2.20) of the same reference, which is equivalent to Eq. (2.1) of the present paper. The derivation of Eq. (2.1) does not replace nuclei a and b by single particles, as is the case in some treatments. As in BE-I the relevant properties of the many-body systems composed of all the nucleons in a and in b interacting with each other as well as with c determine the barrier penetrability parameter β . The possibility of describing the collision between a and b by means of a local and static potential is of course also not fully justifiable for several reasons. In the first place virtual Coulomb excitation and other excitations of nucleons and of collections of nuclei to virtual states produce effects on the forces between a and b that are not accurately describable by a local static potential. Secondly, as long as a transfer of a nucleon between a and b is possible there are forces between a and b arising from the exchange of c as well as from the interchange of identical nucleons. Neither of these forces is rigorously describable by a static local potential. A description by a real potential is of course impossible if reactions and excitations of a and b take place as is the case for reactions. These remarks and cautions have their origin in the impossibility of making a sharp distinction between collisions in which $a+c$ makes no contact with b in the initial stage of the reaction or a makes no contact with $b+c$ in its final stage and collisions in which such contacts take place.

In view of the simultaneous presence of several reactions, the potential V_{ab} will be taken complex. The difference between the procedure used here and that in the usual optical model is that the main part of the transfer of c takes place from positions of a in which its surface is not in contact with that of b so that the main part of V_{ab} is the Coulomb potential. Had it proved necessary to use a strongly attractive V_{ab} at short distances, such a picture would be inapplicable, since an appreciable interpenetration of a and b would result, making the many-body considerations for β loose validity. Large fractions of the total transfer yield would then arise from the complicated interactions of many particles in which the original structures of a and b would lose significance. In the application described below V_{ab} is sufficiently repulsive at short distances to make the main contribution to the transfer probability come from distances for which there is no contact between the nuclear surfaces. The change of V_{ab} from its purely Coulombian value enters the description mainly as a device for obtaining an improvement in the values of the wave function describing the relative

¹⁴ G. Breit, Rev. Mod. Phys. 23, 238 (1951).

motion of a with respect to b for distances at which no contact between a and b is taking place.

The treatment is thus largely free from the objectionable feature of relying on predictions of a model for situations in which the model has little meaning, as would be the case if the ordinary optical model were used. In the calculations to be discussed use is made of the possibility of characterizing the behavior of the many-body problem presented by all of the particles in a and the particle c by means of quantities related to reduced widths as has been done in Refs. 1 and 3. In this respect the treatment has no similarity to the usual optical-model calculations.

The present treatment does not take into account the effect of spin-orbit coupling except for the shell-model considerations in BE-I. One may look accordingly for solutions of (2.1) corresponding to the same total angular momentum $L\hbar$ by setting

$$\bar{\psi}_u^L = \mathfrak{F}^u(\mathbf{r})Y_{Lm}(\theta, \varphi)/r, \quad \bar{\psi}_v^L = \mathfrak{F}_v^v(\mathbf{r})Y_{Lm}(\theta, \varphi)/r, \quad (2.2)$$

where θ, φ are polar angles describing the orientation of \mathbf{r} . The polar axis is chosen along the line joining the centers of mass of the colliding particles, the positive direction being from a to b as in Ref. 3. Substitution into (2.1) gives, then,

$$\left\{ \begin{aligned} \frac{d^2}{dr^2} - \frac{L(L+1)}{r^2} + \frac{2\mu}{\hbar^2}[E - \bar{E}^a - V_{ab}] \right\} \mathfrak{F}_L^u + \frac{\mu}{M}\beta\mathfrak{F}_L^v = 0, \\ \left\{ \frac{d^2}{dr^2} - \frac{L(L+1)}{r^2} + \frac{2\mu}{\hbar^2}[E - \bar{E}^b - V_{ab}] \right\} \mathfrak{F}_L^v + \frac{\mu}{M}\beta\mathfrak{F}_L^u = 0. \end{aligned} \right. \quad (2.3)$$

It may be noted that strictly speaking two coordinate systems such as in BE-II should be used, one corresponding to the initial and the other to the final stage of the process. The quantity \mathbf{r} is $\mathbf{r}_b - \mathbf{r}_{a+c}$ for the first stage and $\mathbf{r}_{b+c} - \mathbf{r}_a$ for the second, in an obvious notation. Since particle c is relatively light the approximation of neglecting the difference between the two kinds of \mathbf{r} is made at this point. Since β is a function of \mathbf{r} , an exact treatment of these coupled equations would be involved. Its value is questionable because the conditions which lead to comparable values of \mathfrak{F}_L^u and \mathfrak{F}_L^v correspond also to the participation of other reaction channels—some open and some closed. For this reason the equations are treated only approximately, the main assumption being that $\bar{\psi}^u$, which corresponds to the incident wave, dominates over $\bar{\psi}^v$. Barring special circumstances such as a resonance, the same relationship holds then also for \mathfrak{F}_L^u and \mathfrak{F}_L^v . The former of these quantities may be obtained in first approximation as

$$\mathfrak{F}_L^u \approx \mathfrak{F}_L^a, \quad (2.4)$$

where \mathfrak{F}_L^a is r times the radial wave function in the expansion of the incident wave, for which c is attached

to a . The expansion has the well-known form

$$\bar{\psi}_u \approx \bar{\psi}_a = \sum_L i^L (2L+1) P_L(\cos\theta) e_L^a \mathfrak{F}_L^a(k_a r)/(k_a r), \quad (2.5)$$

where

$$e_L^a = \exp(i\sigma_L^a), \quad \sigma_L^a = \arg \Gamma(L+1+i\eta_a). \quad (2.6)$$

Here $\eta_a = Z_a Z_b e^2 / \hbar v_a$ is the Sommerfeld parameter for the collision of two charged particles with charges Z_a and Z_b , and v_a is the relative velocity of the two particles. The value of the wave number $k_a/(2\pi)$ entering Eq. (2.5) is that corresponding to the initial state in which $a+c$ moves as a whole with respect to b under the influence of the Coulomb law of force. In order that (2.5) should represent the Coulomb modification of a plane wave of unit density plus a purely outgoing wave at $r = \infty$ it is necessary to set

$$\begin{aligned} \mathfrak{F}_L^a(k_a r) &= \bar{F}_L^a(k_a r) \exp(i\delta_L^a), \\ \bar{F}_L^a &= F_L^a \cos\delta_L^a + G_L^a \sin\delta_L^a, \end{aligned} \quad (2.7)$$

except for a common factor of absolute value for all \mathfrak{F}_L^a . Here $F_L^a(k_a r)$, $G_L^a(k_a r)$ are the usual regular and irregular Coulomb functions. These equations hold for values of r larger than those for which V_{ab} differs appreciably from the Coulomb potential. For smaller values of r , \bar{F}_L^a may be obtained by continuation employing the radial equation. Employment of \mathfrak{F}_L^a in place of \mathfrak{F}_L^u in the second of the two equalities of (2.3) together with the requirement that \mathfrak{F}_L^v be purely outgoing at $r = \infty$ determines the latter function uniquely. From the second line of (2.3), employing the approximation (2.4), it follows by standard methods that

$$\begin{aligned} \mathfrak{F}_L^v(k_b r) &\approx [\mu/(k_b M)] \int_0^\infty \mathfrak{F}_L^b(k_b r') \\ &\quad \times \mathfrak{F}_L^b(k_b r') \beta(r') \mathfrak{F}_L^a(k_a r') dr' \\ &\sim [\mu/(k_b M)] \mathfrak{F}_L^b(k_b r) \int_0^\infty \mathfrak{F}_L^b(k_b r') \beta(r') \\ &\quad \times \mathfrak{F}_L^a(k_a r') dr', \end{aligned} \quad (2.8)$$

where the last form applies only if r is greater than any r' for which $\beta(r')$ is sensibly different from zero. The smaller and larger of the two quantities r and r' are written here as $r_<$ and $r_>$, respectively. Omitting superscripts $\mathfrak{F}_L(\rho) = \mathfrak{G}_L(\rho) + i\mathfrak{F}_L(\rho)$ with \mathfrak{G}_L satisfying the same second-order radial equation as \mathfrak{F}_L and having the asymptotic form $\mathfrak{G}_L \sim \cos\varphi_L$ if $\mathfrak{F}_L \sim \sin\varphi_L$. Substituting $\mathfrak{F}_L^v(k_b r)$ for $\mathfrak{F}_L^u(k_a r)$ in (2.5) and making use of the asymptotic form

$$\mathfrak{F}_L^b(k_b r) \sim \exp\{i[k_b r - (L\pi/2) - \eta_b \ln(2k_b r) + \sigma_L^b + \delta_L^b]\}, \quad (2.8')$$

there is obtained the asymptotic form

$$\begin{aligned} \bar{\psi}_v \sim & \frac{\mu \exp\{i[k_b r - \eta_b \ln(2k_b r)]\}}{k_a k_b M r} \sum_{L=0}^{\infty} (2L+1) P_L(\cos\theta) e_L^a e_L^b \exp[i(\delta_L^a + \delta_L^b)] \int_0^{\infty} \mathcal{F}_L^b(k_b r') \beta(r') \bar{F}_L^a(k_a r') dr' \\ & = \frac{\mu \exp\{i[k_b r - \eta_b \ln(2k_b r)]\}}{4\pi M r} \left\{ I_{\beta^{c(-,+)}(\theta)} + \frac{4\pi}{k_a k_b} \sum_0^{L_m} (2L+1) P_L(\cos\theta) e_L^a e_L^b \right. \\ & \quad \left. \times \int_0^{\infty} \{ \mathcal{F}_L^b(k_b r') \bar{F}_L^a(k_a r') \exp[i(\delta_L^a + \delta_L^b)] - F_L^b(k_b r') F_L^a(k_a r') \} \beta(r') dr' \right\}, \quad (2.9) \end{aligned}$$

where

$$I_{\beta^{c(-,+)}(\theta)} = \int \psi_b^{(e)j(-)*}(\mathbf{r}') \beta(r') \psi_a^c(\mathbf{r}') d\mathbf{r}' = \frac{4\pi}{k_a k_b} \sum_0^{\infty} (2L+1) e_L^a e_L^b P_L(\cos\theta) \int_0^{\infty} F_L^a(k_a r') \beta(r') F_L^b(k_b r') dr'. \quad (2.10)$$

The second of the two asymptotic forms for $\bar{\psi}_v$ in Eq. (2.9) is written in terms of the quantity $I_{\beta^{c(-,+)}(\theta)}$, which is expressed in Eq. (2.10) in terms of an integral involving the ingoing modification of the Coulomb field modified plane wave of unit density in the final state, $\psi_b^{(e)j(-)}$, and the outgoing modification of the Coulomb field modified plane wave of unit density in the initial state, ψ_a^c . This integral differs only through the presence of factors that may be taken outside the integral sign from the $I_0(\theta)$ of Eq. (2.1) of Ref. 8, which is the same as the $I_0(\theta)$ of Eq. (48.27) of Ref. 15 and may be evaluated either by the methods described in these references or, if a high-speed electronic computer is available, by means of the first form for $\bar{\psi}_v$ in Eq. (2.9) employing undistorted Coulomb field radial wave functions. The maximum L for which the radial integrals in Eq. (2.9) sufficiently affected by the differences $\mathcal{F}_L^b - F_L^b$, $\mathcal{F}_L^a - F_L^a$ to make it necessary to take these inequalities into account is denoted by L_m .

The phase shifts δ_L^a , δ_L^b need not be real, the derivations being unaffected by the employment of a finite number of complex phase shifts. The origin of the imaginary part is mainly the presence of other reactions, although strictly speaking the transfer reaction itself calls for complex values of the δ_L . The phase shifts will be considered as complex therefore. However, since the reaction channels responsible for the absorption of the incident wave are not explicitly included in the calculations, the treatment must be regarded as incomplete.

If neither the incident particles nor the reaction products are identical, the differential cross section for the emergence of $b+c$ at angle θ is obtainable from (2.9). It is convenient to write it in the form

$$\bar{\psi}_v \sim \frac{\mu \exp\{i[k_b r - \eta_b \ln(2k_b r)]\}}{4\pi M r} I_{\beta, \text{eff}}^{(-,+)}(\theta), \quad (2.11)$$

where $I_{\beta, \text{eff}}^{(-,+)}$ stands for the quantity in curly

braces in (2.9). The differential cross section is then

$$\sigma_{\Omega}^{NI}(\theta) = \frac{v_f}{v_i} \left(\frac{\mu}{4\pi M} \right)^2 |I_{\beta, \text{eff}}^{(-,+)}(\theta)|^2, \quad (2.12)$$

the superscript NI indicating that all particles have been taken as nonidentical. If, as in the case of $^{14}\text{N}(^{14}\text{N}, ^{13}\text{N})^{15}\text{N}$ the incident particles are identical, a more detailed consideration is needed. On the special assumptions of extreme j - j coupling in the p shell and the exclusive participation of p states in the transfer process, Eq. (16.7) of (BE-I) together with the considerations following it at the end of Sec. IV of that paper result in the application of an additional factor $\frac{1}{4}$ to the right-hand side of (16.7) in BE-I. Transcribing these results to the calculation of the differential cross section including the observation of ^{13}N in the form of so-called "recoils," i.e., the result of transfers from right to left as well as those from left to right,

$$\begin{aligned} \sigma_{\Omega}(\theta) = & \frac{v_f}{2v_i} \left(\frac{\mu}{4\pi M} \right)^2 \\ & \times \{ |I_{\beta, \text{eff}}^{(-,+)}(\theta)|^2 + |I_{\beta, \text{eff}}^{(-,+)}(\pi - \theta)|^2 \\ & - \frac{2}{3} \text{Re}[I_{\beta, \text{eff}}^{(-,+)*}(\theta) I_{\beta, \text{eff}}^{(-,+)}(\pi - \theta)] \}. \quad (2.13) \end{aligned}$$

The total cross section is obtained as

$$\sigma^{\text{tot}} = \int \sigma_{\Omega}(\theta) d\Omega, \quad (2.14)$$

the integration being carried out over all solid angles. In the rather good approximation of neglecting the last term in curly braces in Eq. (2.13), σ^{tot} is contributed to equally by the first two terms, so that

$$\sigma^{\text{tot}} \approx \frac{v_f}{v_i} \left(\frac{\mu}{4\pi M} \right)^2 \int |I_{\beta, \text{eff}}^{(-,+)}(\theta)|^2 d\Omega. \quad (2.15)$$

The last equation corresponds to the statements at the end of p. 697 and beginning of p. 698 in BE-I, since

¹⁵ G. Breit, in *Handbuch der Physik*, edited by S. Flügge (Springer-Verlag, Berlin, 1959), Vol. 41, Part 1, Sec. 48.

(2.15) is just what would follow from (2.12) if one were to forget about spin, statistics, possibility of transfer in two directions, the special p -shell configurations and the simultaneous observation in the direction (θ, φ) of directly produced as well as the recoil type ^{18}N and naively calculated the transfer of the \bar{u} to \bar{v} type. The relationship of the two results just referred to is described above in almost the same words as in BE-I, except that in the latter reference the equations corresponding to (2.12), (2.13), and (2.15) were not explicitly written down.

III. FITS TO DATA

An attempt was made to fit available measurements of the differential and total cross sections of the $^{14}\text{N}(^{14}\text{N}, ^{18}\text{N})^{15}\text{N}$ reaction and of the elastic-scattering cross sections of ^{14}N by ^{14}N in a mutually consistent way. As in Ref. 13, the long-range part of the interaction potential was supposed to be derivable from the representation of nucleon-nucleus scattering data by means of the optical nucleon-nucleus potential to within a factor independent of the nucleus-nucleus distance r . As shown in Ref. 13, this view makes it possible to calculate the long distance tail of the optical potential of the two colliding nuclei, ^{14}N - ^{14}N in the present case, provided the proportionality constant is known. This constant depends on the reduced widths of the nucleons in the ground state of ^{14}N and is approximately proportional to the reduced width of the p -shell nucleons. The present paper makes use of the results of McIntosh, Park and Rawitscher¹³ regarding the space dependence of the tail of the ^{14}N - ^{14}N potential and the factor connecting this potential with the reduced width. The value of the reduced width is adjusted, however, so as to agree not only with ^{14}N - ^{14}N scattering but also with the total cross section of $^{14}\text{N}(^{14}\text{N}, ^{18}\text{N})^{15}\text{N}$.

The analysis of elastic-scattering data suffers from the following complications. On account of the identity of the projectile and target it is not possible to separate effects of distant from close collisions by using small angle data. The elastic scattering at low energies is dominated by Coulomb effects making the determination of purely nuclear effects difficult. As in Ref. 13 it proved impossible to rely entirely on the ^{14}N - ^{14}N potential in the region of r large enough to make the derivation of the long distance tail of the ^{14}N - ^{14}N potential valid. It was necessary therefore to join the tail to a phenomenological optical potential at smaller r . The optical potentials at shorter distances have, however, no theoretical justification. On the other hand, since it proved possible to account for elastic scattering as well as for the neutron-transfer reaction by the same optical potential, the data fitting is not as arbitrary a procedure as that used in many other applications of this phenomenological device. The reduced neutron widths needed for neutron transfer and for elastic scattering also appear to be reconcilable or at least not

contradictory. In this respect there appears to be no reason for suspecting the consistency of the explanation. It should be emphasized, however, that for neutron transfer two different potentials should be used: one for the initial $^{14}\text{N}+^{14}\text{N}$ arrangement of nucleons and another for the final $^{18}\text{N}+^{15}\text{N}$ rearranged grouping of nucleons. Since no data on the elastic scattering of ^{18}N by ^{15}N are available, the potential in the final arrangement was taken to be the same as in the initial one. It is not known that the difference between the initial and final potentials is small enough to make the error introduced negligible. On the other hand, the authors are not aware of a reason for supposing the difference between the two potentials to be large enough to affect the main conclusions arrived at in this paper.

In the calculations on neutron transfer the quantity $\beta(r)$ of the preceding section was set equal to zero for $r < r_{\text{cut}}$ with preassigned values of the cutoff distance r_{cut} . The reason for doing so is that if the spatial nucleon distributions of the colliding nuclei interpenetrate, there is an increase in the probability of other reactions. The competition between the neutron-transfer reaction and the definitely exothermic ones such as $^{14}\text{N}(^{14}\text{N}, ^{12}\text{C})^{16}\text{O}$ may then be expected to inhibit the neutron transfer. The value of r_{cut} was used as one of the adjustable parameters and stayed around 7.2 F, a value corresponding approximately to contact between the nuclei with somewhat larger than usual nuclear radii. The sharp cutoff is not expected to represent the actual situation accurately. It would have been possible to use a gradual decrease of $\beta(r)$ to 0 as r decreases. It is believed, however, that the resulting gain in realism would not be an essential one because of the omission of other effects, such as the energy dependence of the parameters entering the potential and more generally its nonlocal character, the shortcomings³ of the two-state energy matrix approximation of transfer theory, the omission of the dynamic reaction terms, etc. The use of the cutoff for $\beta(r)$ is in qualitative agreement with the rounding off of the usual plot of the logarithm of total cross section against energy at energies definitely above the Coulomb barrier for many transfer reactions.

The calculations of the differential and total cross sections of the neutron-transfer reaction made use of the equations of Sec. II by means of two machine programs written for the IBM 7094 electronic digital computer. The numerical work was carried out on the IBM 7094-7040 direct coupled system at the Yale Computer Center. The first program provided values of the Coulomb functions¹⁶ and their derivatives. Employing the values of these functions the second program¹⁷ was used to obtain $I_{\beta, \text{eff}}^{(-,+)}$ at needed values of θ . The

¹⁶ In preliminary stages of the work a FAP Coulomb Functions machine program written and kindly lent by Dr. G. H. Rawitscher was made use of in debugging the Fortran IV program used in the calculations reported on in this paper.

¹⁷ Dr. J. S. McIntosh collaborated in writing parts of the initial version of this program.

proportionality constant of $\beta(r)$, i.e., the quantity $1/\lambda_1\lambda_2$ of BE-I was adjusted by that program to give the best fit to the experimental values by minimizing χ^2 , the weighted sum of squares of deviations of calculated from observed values. The same values of the fundamental constants were used as in Ref. 8. It was ascertained by trial that the first twenty values of L are sufficient for the calculation of the series for $I_{\beta, \text{eff}}^{(-,+)}$. The addition of higher L values affects the results by less than 1%. Tests of the adequacy of this approximation were made periodically as new potentials were tried, the usual sequence of the maximum L included in a test case being 22, 25, 27, 30.

The absence of a significant accumulation of rounding-off errors in the evaluation of the sum over L representing $I_{\beta}^{(-,+)}$ was ascertained by comparing the values of the real, imaginary and absolute values of $I_{\beta}^{(-,+)}$ and of σ_0 with those obtained by means of Eqs. (6.1) to (6.4) of Ref. 3 in terms of the hypergeometric function ${}_2F_1$, in the case of a Coulomb field and a reaction with vanishing Q value. The possibility of evaluating the sum over L up to a moderately small maximum value of L , say L_m , subtracting the value of that sum for a Coulomb potential and adding the value of the sum up to $L = \infty$ for a Coulomb interaction along the lines of Eq. (2.9) was examined. Its advantages in decreasing uncertainties arising from the use of many terms of the series over L appeared outweighed by the greater complexity of the machine program. The equation is nevertheless included in the present report on account of its possible usefulness in desk machine calculations. It was used to provide a check on the partial-wave machine program. In the main data fitting, that program was used with $\mathcal{F}_L^a = \mathcal{F}_L^b \equiv \mathcal{F}_L$ at a common center-of-mass energy $E_i + Q/2$, where E_i is the incident center-of-mass kinetic energy. This approximation is suggested by the smallness of the Q value of the reaction. The accuracy of the approximation was tested by comparison with calculations in which \mathcal{F}_L^a and \mathcal{F}_L^b were used with \mathcal{F}_L^a corresponding to the incident energy E_i and \mathcal{F}_L^b to the energy $E_i + Q$. These comparisons indicated a 2% accuracy of the approximation, an accuracy believed sufficient in view of the experimental uncertainties.

In the approximation of using $E_i + Q/2$ in place of E_i and $E_i + Q$ it is seen from (2.10) that

$$I_{\beta, \text{eff}}^{(-,+)}(\theta) = (4\pi/k^2) \sum_{L=0}^{\infty} (2L+1) e_L P_L(\cos\theta) \times \int_0^{\infty} \mathcal{F}_L^2(kr) \beta(r) dr, \quad (3.1)$$

in the notation of the preceding section. In the absence of a nuclear potential \mathcal{F}_L becomes the regular Coulomb function F_L . In this case Eq. (3.1) gives values agreeing with the steepest descents approximation used by BCW to within a few percent and practically perfectly with the hypergeometric function written out in Ref. 3.

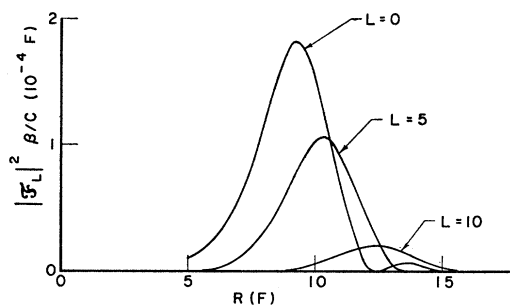


FIG. 1. $|\mathcal{F}_L|^2 \beta/C$ corresponding to potential 1 for $L=0, 5, 10$. Effects for $R < 5$ F are seen to be small for most L .

Figure 1 shows plots of $|\mathcal{F}_L^2(kr)|\beta(r)$ against r for several values of L . The main contribution to the integral in (3.1) is seen to arise from the region $r > 5$ F. For further details reference is made to the figure legend. The integration was started therefore at $r = 5$ F. It will be noted that this integral is proportional to the first Born approximation to the phase shift if $\beta(r)$ is replaced by the potential. Since $\beta(r)$ decreases with r while the potentials used are nearly constant for small r , the region $r < 5$ F is also not important for phase-shift calculation. The main contributions to the integrals in (3.1) arise from the vicinity of the classical turning point in agreement with the general connection¹⁵ between the semiclassical approximation and the quantum treatment.

The potential energy V_{ab} of the preceding section was used in the form

$$V_{ab} = (Z_1 Z_2 e^2/r) + V + iW \quad (r \geq 5 \text{ F}) \quad (3.2)$$

for values of r greater than the somewhat arbitrarily chosen value $r = 5$ F and continued as a constant $V_{ab}(r = 5 \text{ F})$ through $r \leq 5$ F. The quantities V and W are real, W taking account of the absorption of the wave caused by reactions competing with elastic scattering. No attempt was made to refine the calculation by using a rounded modification of the Coulomb potential represented by the first term on the right-hand side of (3.2). Such a modification would take into account more realistically the probable space distribution of the proton density. It was not used because the region $r \leq 5$ F is accessible only to a few partial waves with small L and because the effective potential between the colliding nuclei is at best only a schematic representation of a many-body interaction that cannot be pictured correctly in three dimensions. Saxon-Woods-type potentials were used for V and W in the following notation:

$$V = V_0 / \{1 + \exp[(r - r_v)/a_v]\}, \quad (3.3a)$$

$$W = W_0 / \{1 + \exp[(r - r_w)/a_w]\}. \quad (3.3b)$$

In the limit $r \gg r_v$, Eq. (3.2a) becomes

$$V = [V_0 \exp(r_v/a_v)] \exp(-r/a_v) \quad (r \rightarrow \infty). \quad (3.4)$$

Calculations of V performed¹³ in the adiabatic approxi-

TABLE I. Values of parameters of three potentials.

Potential number	V_0 (MeV)	r_v (F)	a_v (F)	W_0 (MeV)	r_w (F)	a_w (F)	r_{cut} (F)
1	-3.6	6.2	0.543	-2.2	8.3	0.27	7.1
2	-1.5	7.8	0.543	-2.0	7.8	0.50	7.2
3	-1.73	8.0	0.543	-1.98	7.83	0.511	7.2

mation give $a_v=0.543$ F. The factor $V_0 \exp(r_v/a_v)$ in (3.4) is proportional to the neutron reduced width.

As mentioned earlier in this section, the calculations were made as though V_{ab} were the same in the initial and final states of the neutron-transfer reaction. It may also be mentioned that the introduction of a phenomenological potential describing the ^{13}N - ^{15}N interaction would increase the number of parameters available. Therefore, unless the relationship of the ^{13}N - ^{15}N and ^{14}N - ^{14}N potentials, such as their difference, should become sufficiently well known from other sources of information, the fits to data could be improved by the introduction of the second complex potential but without assurance that the improvement has a physical significance.

In the later stages of the work three potentials with parameters recorded in Table I were under consideration for the representation of neutron-transfer data. Potential 1 is nearly the same as that used in the fit presented at the 1964 Paris Conference¹⁸ except for $r_{\text{cut}}=0$ and a variable r_w decreasing with increasing E having been used in the earlier report.¹⁸ The variation in r_w came about in attempting to fit older differential cross-section data at¹⁹ 18.0 MeV, but proved unnecessary when newer data were used instead. The neutron reduced width derived from transfer data was found to increase with E by amounts greater than could be ascribed to statistical uncertainties. In the older work¹⁸ the real parts of the potentials were the same for neutron transfer and elastic scattering but the imaginary parts were not. Potential 2 was designed to remove the necessity of systematic variations in reduced width in fitting transfer data and to account simultaneously for neutron transfer and elastic scattering. Potential 3 gives good fits to neutron-transfer data employing a constant reduced width but does not fit elastic scattering unless r_w is reduced from its present value by about $1F$. The small r cutoff of $\beta(r)$ was used in neutron-transfer but not in elastic-scattering calculations.

The neutron-transfer differential cross-section data are intended to supply relative values at any one energy. The adjustment of theory to experiment was made therefore with the following end in view. The quantity $\beta(r)$ was expressed as

$$\beta(r) = C e^{-\alpha r} / r. \quad (3.5)$$

¹⁸ G. Breit, J. A. Polak, and D. A. Torchia, in *Proceedings of the Congrès International de Physique Nucléaire, Paris, 1964* (Editions du Centre National de la Recherche Scientifique, Paris, 1965).

¹⁹ The energy of the projectile in the laboratory system is used throughout this paper in referring to experimental data.

Denoting the parameters entering a given form of the potential by $a_1, a_2, \dots, a_p, \dots, a_n$ one has

$$V_{ab} = V_{ab}(r; a_1, a_2, \dots, a_p, \dots, a_n) \quad (3.6)$$

and

$$\sigma_\Omega = C^2 \sigma_\Omega^{(1)}(\theta, E; a_1, a_2, \dots, a_p, \dots, a_n). \quad (3.7)$$

With the parametrization used in Eqs. (3.2) to (3.4) the parameters a_p are V_0, r_v, a_v, W_0, r_w , and a_w , but for more general forms a larger number of parameters would come under consideration. Considering neutron-transfer data alone, the best adjustment of C and of the a_p to the data corresponds to minimizing the weighted sum of squares of deviations:

$$\chi^2 = \sum_E \sum_{i=1}^{n_E} w_i [B_E \sigma_\Omega^{(1)}(\theta_i, E; a_p) - \sigma_{\Omega, m}(\theta_i, E)]^2 + \sum_j W_j [C^2 \sigma^{\text{tot}(1)}(E_j; a_p) - \sigma_m^{\text{tot}}(E_j)]^2, \quad (3.8)$$

with respect to independent variations of C^2 , the a_p and the B_E . The values of θ at which measured values at energy E are available are here denoted by θ_i with $i=1, 2, \dots, n_E$ and the measured values of σ_Ω by $\sigma_{\Omega, m}(\theta_i, E)$; the measured values of σ^{tot} at energy E_j are designated by $\sigma_m^{\text{tot}}(E_j)$ and the corresponding theoretical values by $C^2 \sigma^{\text{tot}(1)}$. Superscript (1) in (3.7) and (3.8) indicates evaluation for $C=1$. The weights w_i and w_j are related to the "standard errors" $\Delta \sigma_{\Omega, m}(\theta_i, E)$ and $\Delta \sigma_m^{\text{tot}}(E_j)$, i.e., the experimental uncertainties expressed as standard deviations of supposedly "normal distributions," by

$$w_i = 1 / [\Delta \sigma_m(\theta_i, E)]^2, \quad W_j = 1 / [\Delta \sigma_m^{\text{tot}}(E_j)]^2. \quad (3.9)$$

The usual hypothesis of absence of error correlations in the measurements is implied in the above statement of the data-analysis problem. There is room for doubt regarding its actual applicability since the $\sigma_{\Omega, m}(\theta_i, E)$ may be systematically off in one or another direction for a few neighboring θ_i at given E as compared with values in another range of θ . Similarly a systematic source of error may make the $\sigma_m^{\text{tot}}(E_j)$ too high or too low for a few neighboring E_j as compared with values for another E_j . In view of these uncertainties regarding the applicability of usual assumptions in the statistics of data treatment as well as the approximate character of the theory combined with relative recency of stabilization of experimental values, a complete treatment in terms of Eq. (3.8) was not attempted, but that equation was nevertheless useful as a guide.

The absence of C in the first sum occurring in Eq. (3.8) makes it possible to test any assumed potential for constancy of the value of C needed to represent neutron-transfer data without using directly the angular distribution information. For this reason, least-square fits to the σ_m^{tot} data were made by means of a polynomial in the energy representation of $\ln \sigma^{\text{tot}}$ as follows:

$$\sigma^{\text{tot}}(E) = \exp(a_0 + a_1 E + a_2 E^2 + \dots). \quad (3.10)$$

The best values of the coefficients of E in the polynomial were determined. The data of Hiebert, McIntyre and Couch⁵ (HMC) and those of Gaedke, Toth, and Williams⁶ (GTW) have been separately represented in this way with rather similar results, especially at energies above $E_l=11$ MeV. The least-squares fits were made employing the second term in Eq. (3.9) and replacing the term proportional to C^2 in square brackets by the exponential function appearing on the right-hand side of Eq. (3.10). Polynomials of various degrees were tried. A quartic appears to provide a satisfactory fit without overparametrization, as seen in Fig. 2. In this figure three sets of curves are shown, the upper set referring to the HMC, the next below to the GTW data and the lowest to the comparison of the potential 3 and BCW (pure Coulomb potential) theoretical curves. For the lowest set the normalization is arbitrary but adjusted to give osculating joining at low E . In the upper two sets of curves the quartic fits to each of the two sets of data are shown as dashed curves, the theoretical energy dependence for potential 1 by circles, for potentials 2 and 3 by a full curve. In all cases the theoretical curves, whether fully drawn or indicated by points, have been adjusted to give a minimum χ^2 to the full set of data with which they are compared. The relationship of the fits to each other and to the data is displayed on an expanded scale for the laboratory-energy range 16–19.5 MeV in the inset at the lower

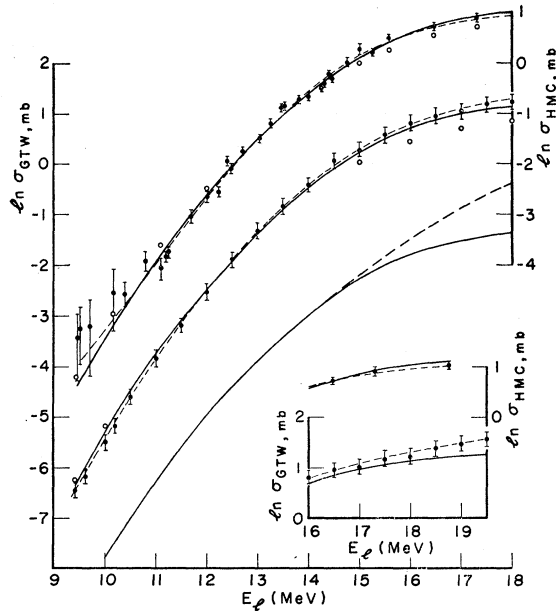


FIG. 2. Total cross-section data of HMC and GTW are shown by the upper and lower sets of data points, respectively. Fits obtained employing potentials 2 and 3, which are identical to within the accuracy of the drawing, are shown by solid curves. Other conventions: open circles for fit obtained with potential 1; light dashed curves for quartic fits; full line in lowest part of main figure is the potential 3 curve displaced downwards in order to compare with heavy dashed curve representing pure Coulomb case in BCW approximation. Inset at lower right shows extension of fits to 19.5 MeV.

TABLE II. Comparison of the goodness of fit of the three potentials to neutron-transfer data at the angular distribution energies.

Potentials:			1		2		3	
E_l (MeV)	n_E	ΔC_E (F ⁻¹)	D	C_E (F ⁻¹)	D	C_E (F ⁻¹)	D	C_E (F ⁻¹)
11.0	19	0.41	1.5(5)	13.2	1.5(5)	13.2	1.5(5)	13.0
12.3	35	0.23	1.0	13.3	1.0	13.5	1.0	13.3
13.24	34	0.17	1.3	14.8	1.0	14.1	1.0	13.0
14.0	38	0.18	1.1	15.5	1.1	14.4	1.1	14.0
16.0	40	0.28	0.9(5)	16.4	1.0	14.0	0.8	13.7
[$\langle C^2 \rangle^{1/2} / C_{sp}$] _{HMC}			0.98 ± 0.04		0.92 ± 0.03		0.90 ± 0.03	
[$\langle C^2 \rangle^{1/2} / C_{sp}$] _{GTW}			1.04 ± 0.08		0.99 ± 0.08		0.97 ± 0.08	

right. Potentials 2 and 3 are seen to give fits of comparable quality and to come close to the quartic fit. The lowest set of curves shows close similarity of energy dependence for potential 3 with that for the purely Coulomb case at the lower but not at the higher E . The imaginary part of the optical potential depresses the yield at the higher E .

In adjustments of the potential parameters the quartic fit values corresponding to the σ_m^{tot} of HMC at the energies for which angular distributions are available were employed. No account was taken in these adjustments of the presence of error correlations between the $\sigma^{\text{tot}}(E)$ as obtained at these energies by the quartic fit which exist even if the $\Delta\sigma_m^{\text{tot}}(E_j)$ are uncorrelated. This error correlation may be expected to be rather strong but, since the results of the adjustments reported on here do not pretend to give more than an approximation to the best possible representation of available data and for other reasons mentioned previously, the error introduced is believed not to affect the reliability of conclusions materially. Through the employment of these $\sigma^{\text{tot}}(E)$ the calculation of phase shifts from potentials had to be done only at the energies E of the first term of Eq. (3.8) for which angular distributions are available. In effect, at each such energy there were then available absolute values of σ_n which were fit by allowing $V_0, r_v, W_0, r_w,$ and a_w to vary. The additional requirement of an energy-independent C^2 was imposed. The fits carried out were obtained mainly by cut and try procedures. The adjustment of potential 3 to neutron-transfer data was made more systematically with potential 2 as a starting point. With values of other parameters kept fixed, one a_p of (3.6) was varied at a time adjusting it to its best value at a particular E , taking the weighted average of the changes in that a_p to determine the change to be used before going on to variations of the next parameter. The potential giving best over-all agreement with neutron-transfer and elastic-scattering data was obtained, however, primarily by a cut and try rather than by a systematic procedure.

The goodness of fit to neutron-transfer data at the energies for which angular distributions are available is compared in Table II. The laboratory energy E_l in

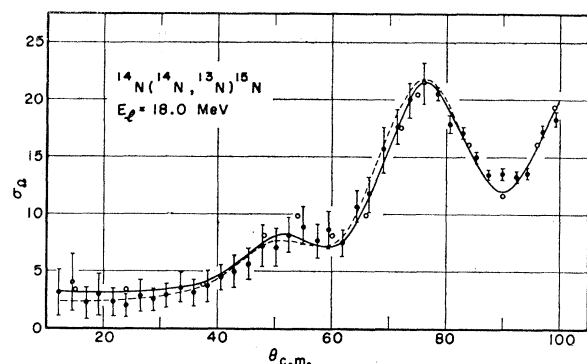


FIG. 3. Fits to relative differential cross-section data of HMC at $E_l = 18.0$ MeV are shown by solid and dashed curves for potentials 2 and 3, respectively. Open circles indicate fit produced by potential 1.

MeV and n_E , the number of angles at which relative values of the differential cross section have been measured, are listed in the first two columns. The third column contains values of ΔC_E , the uncertainty in C_E , the value of C at energy E as determined by the error matrix method for the quartic fit. The listed ΔC_E are for potential 1. The values for other potentials are similar, being proportional to C_E and thus readily obtainable from those listed. The tabulated values of ΔC_E are intended only as a guide for forming a judgment regarding the variability of C_E in the remainder of the table. The presence of correlations in errors at neighboring energies for the quartic fit would not justify, however, regarding the C_E at different energies as having statistically independent uncertainties ΔC_E . At each energy listed in the first column the value of C was found as

$$C_E^2 = \sigma^{\text{tot}}(E) / \sigma^{\text{tot}(1)}(E; a_p), \quad (3.11)$$

where $\sigma^{\text{tot}}(E)$ is the quartic fit value at energy E and other symbols in the same convention as in (3.8). The a_p have different values for different potentials and the values of C_E^2 therefore differ also. At each E_l the weighted mean-square deviation D was calculated by

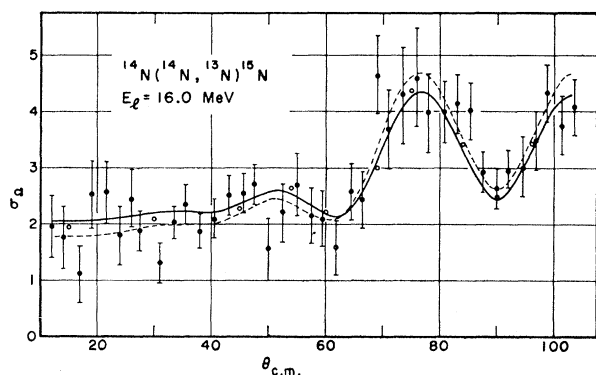


FIG. 4. Fit to relative differential cross-section data of HMC at $E_l = 16.0$ MeV. Conventions as in Fig. 3.

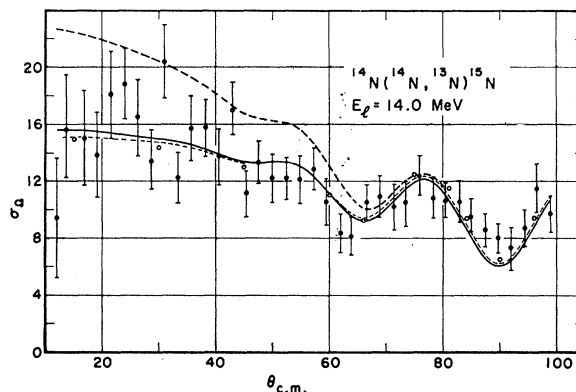


FIG. 5. Fit to relative differential cross-section data of HMC at $E_l = 14.0$ MeV. Heavy dashed curve indicates fit obtained when only the Coulomb interaction between the nuclei is considered. This curve is normalized to the potential 2 result at 90° . Otherwise conventions as in Fig. 3.

adjusting B_E to give a minimum of the contribution of that E to the first term in (3.8) and dividing by $n_E - 1$. The values of D and C_E are listed for the three potentials in the last six columns of the table. At the bottom of the table are given the values of $\langle C^2 \rangle^{1/2} / C_{sp}$ for the three potentials, employing total cross-section data in the range 11.0 to 16.0 MeV directly, without the intermediary use of the quartic fit. The subscript sp indicates that the value of C obtained from the single-particle model is used. The single-particle potential employed in calculating C_{sp} was the same as in the 1964 reference to the work of McIntosh, Park, and Rawitscher¹³ except for a slight adjustment to reproduce the neutron binding energy more accurately. The reduced width was affected by this change by 0.5%, an amount negligible in the comparisons made here. The quantity $\langle C^2 \rangle$ is the weighted mean of the C_E^2 for the potential in question with relative weights

$$w_j^{\text{tot}} \equiv [\sigma_m^{\text{tot}}(E_j) / \Delta \sigma_m^{\text{tot}}(E_j)]^2. \quad (3.12)$$

This weighting follows from minimizing χ^2 , as in (3.8), with respect to C^2 . The energy range used in obtaining

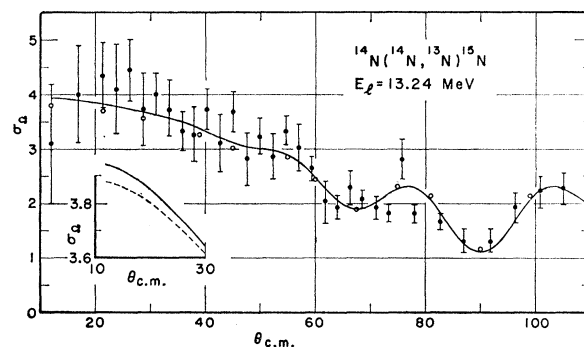


FIG. 6. Fit to relative differential cross-section data of HMC at $E_l = 13.24$ MeV. Inset shows comparison of results for potentials 2 and 3 for the angular range 10° to 30° with the scale magnified by a factor of 5. Otherwise conventions as in Fig. 3.

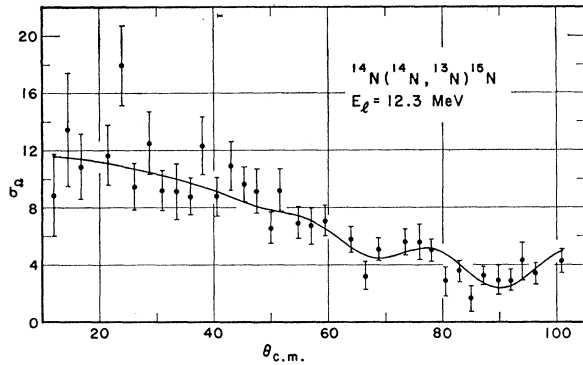


FIG. 7. Common fit for potentials 1, 2, and 3 to relative differential cross-section data of HMC at $E_l=12.3$ MeV.

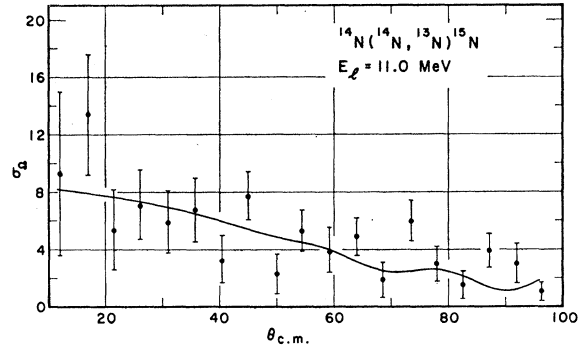


FIG. 8. Common fit for potentials 1, 2, and 3 to relative differential cross-section data of HMC at $E_l=11.0$ MeV.

$\langle C^2 \rangle$ was $11.0 \text{ MeV} < E_l < 16.0 \text{ MeV}$. The two sources of data are referred to by the subscripts HMC and GTW. The procedure used in the determination of the uncertainties in the values of $\langle C^2 \rangle^{1/2}/C_{sp}$ listed in Table II is described in connection with Table V. The comparison of differential cross-section data with relative values expected for the three potentials is shown in Figs. 3-8 at $E_l=18.0, 16.0, 14.0, 13.24, 12.3,$ and 11.0 MeV, respectively. In all cases the value of C used at a particular energy has been adjusted to give the least χ^2 at the energy, as in Table II. Therefore, the fits shown are somewhat better than they would be if energy-independent values of C were used for each potential. The same designations for indicating values corresponding to the potentials are used throughout this set of graphs. The difference in angular-distribution predictions becomes perceptible only at the higher of the six energies. At the lowest two energies the angular distributions are the same as for a purely Coulomb potential, within the accuracy of the drawing. At 14 MeV the effect of removing the non-Coulomb parts is seen in Fig. 5. It increases with increasing energy.

In Table III the goodness of fit to the elastic-scattering differential cross section is compared for the three potentials. The values of D have the same significance as for neutron-transfer data. Columns labeled D' list the values of D corresponding to the values of r_w which give the best fit to elastic-scattering data with the other parameters of Table I kept fixed. These values of r_w are referred to as r_w' in the table. The decrease in D that results from the adjustment of r_w is appreciable in

several instances. However, in most cases D' , the improved D , is less than 1. Since there is no reason for demanding such small values of D these improvements are hardly significant. On the other hand, for potential number 1 and 3, at $E_l=21.7$ MeV, D is decidedly improved by the readjustment of r_w . For potential number 1, $r_w' - r_w = 0.3$ F; for potential 3, $r_w' - r_w = -1.3$ F. The sense of direction of the energy dependence of r_w called for by elastic-scattering data is thus dependent on other potential parameters. For potential 2 the improvement of the fit to data at 21.7 MeV is hardly significant since for the value of r_w as in Table I the excess of D over unity is slight.

IV. DISCUSSION

Comparison of Table III with II shows that although potential 3 gives a slightly better fit to neutron-transfer data than potential 2, it gives a much poorer representation of elastic scattering. Potential 2 is better than potential 1 both for transfer and for scattering. Since differences in D for neutron transfer are small for the three potentials, the preference for potential 2 on this score is not a decided one. The difficulty of assigning figures of merit to the potential is increased by the fact that the incident energies considered for elastic scattering are appreciably larger than those for transfer, the highest energy in Table II being only slightly larger than the lowest in Table III. On the other hand, the applicability of neutron-transfer theory to energies higher than those in Table II is questionable. For example, at $E_l=18.0$ MeV, the distance of closest ap-

TABLE III. Comparison of the goodness of fit of the three potentials to elastic-scattering data.

Potentials:		1			2			3		
E_l (MeV)	n_E	D	D'	r_w' (F)	D	D'	r_w' (F)	D	D'	r_w' (F)
15.0	9	1.0	1.0	7.4	1.0	1.0	7.1	0.9	0.9	7.0
17.7	9	1.1	0.7	7.6	1.0(5)	0.5(5)	7.0	1.4	0.5	6.7(5)
19.2	9	0.7	0.7	8.25	0.7	0.4	7.4	1.5	0.3	6.9(5)
21.7	12	3.0	1.3	8.6	1.1	0.4	7.4	4.2	0.6(5)	6.5

proach on a Rutherford orbit corresponding to $\theta=160^\circ$ is 7.9 F. On account of particle identity, this value of θ enters calculations of neutron-transfer probability at 20° in the center-of-mass system. Since some of the r_v and r_w in Table I are greater than 7.9 F, it is possible that for such collisions the nuclei begin to merge sufficiently to make a picture of two separate nuclei used in this paper inapplicable. The correction for the range of nucleon-nucleon force makes the overlap of the matter distributions not as pronounced as the values of r_v and r_w would indicate but the values of a_v and a_w as well as the lack of sharp localization of the positions of the nuclei give corrections in the opposite direction. Therefore the assurance for the validity of the theory at 18 MeV is questionable but not absolutely excluded.

Employing the values of the reduced width needed to explain the absolute value of the tail of the interaction potential in the work of McIntosh, Park, and Rawitscher and allowing for the ratio in the tail heights of the potentials employed here as compared with those used by them, ratios of elastic-scattering values of reduced widths required for the explanation of the long-range parts of the potentials used here to single-particle reduced widths may be obtained. These are listed in Table IV. The values of C_{sp} used for this table are the same as those for Table II. Comparison of the bottom rows in Table II with Table IV indicates a preference for potential 3, leaving a disagreement in values of the reduced width by roughly a factor of 2. This disagreement as well as the preference for potential 3 over potential 2 are not believed to be especially significant for the following reasons. The adjustment of the depth of the nucleon-nucleus potential in the work on elastic scattering affects the nucleon-nucleus wave function rather strongly. The results are sensitive therefore to the exact way in which the adjustment is made. The necessity of making the adjustment is connected with imperfections of the method used for the calculation of the tail of the potential and this adjustment is more an expedient than a fully justified procedure. Furthermore, the nucleus-nucleus potential is affected by the reduced widths of all nucleon states in the p shell and also in the s shell as well as partly by protons. On the other hand, on the j - j coupling model used in BE-I, neutron transfer is concerned mainly with the transfer of a $p_{1/2}$ neutron. Again, the error committed by disregarding the difference between the effective potentials for

^{14}N - ^{14}N and for ^{13}N - ^{15}N affects neutron transfer and not elastic scattering. It may be noted that McIntosh, Park, and Rawitscher do not consider the reduced width to be determined by their data analysis to much better than a factor of 2. Much of this uncertainty arises from the difficulty of isolating truly long-range collisions which is bound up with the identity of the colliding nuclei and makes it difficult to isolate the effects of the long-range part of the potential. This inherent difficulty in analyzing ^{14}N - ^{14}N scattering affects the present work as well.

The determination of $\langle C^2 \rangle^{1/2}/C_{sp}$ from neutron transfer is also subject to uncertainties which are partly indicated in the last two rows of Table II. In Table V these uncertainties are broken down into parts arising from uncorrelated (statistical) and correlated (systematic) sources of error in total cross-section data. The "uncorrelated" and "correlated" designations have reference to data at different energies. The designation Δ' indicates taking the effect on the uncertainty in the standard deviation convention that is caused by the uncorrelated error; ΔC^2 is the uncertainty in $\langle C^2 \rangle$ obtained by compounding the contributions of uncorrelated and correlated errors in quadrature. The uncertainties $\Delta' C^2$ and ΔC^2 are expressed in percentages of the corresponding C^2 . The energy interval used is shown in the second column of the table in terms of the lower and upper limits of the laboratory energy E_l . In the case of the GTW data it was difficult to assign experimental errors to the two categories with certainty. Somewhat arbitrarily the detection efficiency error of 15% was considered as correlated and the remaining error as uncorrelated. It is practically certain that this division of the total uncertainty of an individual datum underestimates the systematic error and therefore also the value of ΔC^2 . Were the whole error considered as systematic $(\Delta C^2)_{GTW}$ would be 30% of $\langle C^2 \rangle$. Similarly in the case of the HMC data the partial presence of systematic (correlated) errors in the stated errors of individual points that do not include the 7% stated correlated uncertainty also increases the uncertainty of $\langle C^2 \rangle$. The uncertainties in Tables II and V are therefore likely to be underestimates.

Inspection of values of $\langle C^2 \rangle$ derived from the two sources of data shows disagreement by more than 10%.

TABLE IV.* Elastic-scattering values of C/C_{sp} , the ratio of reduced width to its single particle value.

Potential	1	2	3
C/C_{sp}	0.04	0.3	0.5

* The values in this table make use of the effect of the reduced width on the nucleus-nucleus potential in the adiabatic approximation. Since the potential affects elastic scattering somewhat more directly than neutron transfer the values in this table are sometimes referred to as values derived from elastic scattering.

TABLE V. Uncertainties in squares of reduced widths.

Potential	Data E (MeV)	HMC			GTW		
		$\langle C^2 \rangle$	$\Delta' C^2$ (%)	ΔC^2 (%)	$\langle C^2 \rangle$	$\Delta' C^2$ (%)	ΔC^2 (%)
1	(11.0,16.0)	219	1.8	7.2	247	4.6	15.7
2	(11.0,16.0)	195	1.8	7.2	223	4.6	15.7
3	(11.0,16.0)	187	1.8	7.2	215	4.6	15.7
1	(9.4,19.5)	225	1.7	7.2	236	3.3	15.3
2	(9.4,19.5)	193	1.7	7.1(5)	214	3.2	15.3
3	(9.4,19.5)	187	1.7	7.2	211	3.2	15.3

Since the value based on GTW measurements is always the higher, it is likely that there is a difference in the correlated errors in the two cases but further experimental work would be needed to ascertain the total uncorrelated (systematic) uncertainty.

The fractional uncertainty of C^2 is twice that of the reduced width. In the case of the HMC data the latter appears to be between 3.5 and 7%, and in the case of GTW between 7.5 and 15%. Since absolute-value determinations often take appreciable time to settle down, the difference from the true value may be larger than the estimates. Combining these uncertainties in $\langle C^2 \rangle$ from transfer with those in $\langle C^2 \rangle$ from elastic scattering as well as the previously mentioned incompleteness of the theory, there appears to be no reason for regarding the difference between C/C_{sp} of Table IV and $\langle C^2 \rangle^{1/2}/C_{sp}$ of Table II for potential 3 as serious.

The values of the quantity

$$\theta_0^2 = b/(3\lambda),$$

where b is an assumed value of the nuclear radius, have been calculated by Becker and McIntyre.⁵ The ratio to the shell-model value according to their numbers is $(4.5 \pm 1.0)/(5.2 \pm 1.0) = 0.87 \pm 0.26$. According to Table II the comparable values for potentials 2 and 3 are 0.92 ± 0.03 and 0.90 ± 0.03 , respectively. As previously stated the uncertainties may actually be larger. In either case there is no significant disagreement between the numbers in Table II and the ratio following from those of Becker and McIntyre. There are some minor differences in detail, however, which make a direct comparison not too significant. The work in Ref. 5 makes use of a value $\theta_0^2 = 4.5 \times 10^{-2}$ employing the BCW total cross-section formula at $E_l = 13.6$ MeV and the experimental value 0.043 F^2 of the cross section. The value of the cross section at that energy corresponding to calculations in Table II is 0.040 F^2 . It appears that the numbers in Ref. 5 correspond to the energy in the c.m. system without the addition of $Q/2$. Including these refinements the $\theta_0^2 = 0.045$ with $b = 5 \text{ F}$ changes to 0.038 which corresponds to the calculations reported on here. This change would make the ratio of the transfer value

to the shell-model value 0.74 in place of 0.87 . There would still be no disagreement with Table II. The shell-model reduced widths used in the two papers are also different, the ratio of that used here to that used in Ref. 5 being 0.81 . It is perhaps a misnomer to call the single-particle model used here a shell model, because it is primarily designed to represent the approximately exponential decay of the neutron wave function outside the nucleus.

In this respect the theory in BE-I and in the black box point of view of the molecular model is essentially different from that commonly used in discussions of (d,p) reactions. The nucleon configurations used in the former two treatments are those in the peripheral region of the nucleus. The wave functions describing them are simpler than those needed in the nuclear interior. Their important parts can in principle be characterized by relatively few parameters while the shell model wave functions of the usual (d,p) theory are used as though they represent the nuclear wave function throughout the whole nucleus. It is well known that such a representation is quite poor. The picture also lacks realism in the part of configuration space in which two nuclei interpenetrate, and yet this part is used in the calculations. The black box approach also has weak points some of which have been discussed in Ref. 3.

The evidence points on the whole to a smaller value of the reduced width than that corresponding to the escape of particles from a $j-j$ coupled p shell, which was assumed for use with the single-particle reduced width in BE-I. The reduction factor suggested by Table II is small however, indicating considerable simplicity of the peripheral nuclear structure consisting in the dominance of the shell-model configuration over the admixture of other configurations. As previously mentioned, however, the theory has many imperfections.

ACKNOWLEDGMENTS

In addition to the acknowledgments made in Refs. 15 and 16, the authors wish to thank Professor J. A. McIntyre for helpful discussions of experimental data, Dr. E. Hadjimichael for checking some of the calculations, and R. E. Seamon for the loan of a least-squares Fortran IV program.